

ON THE SIZE EVOLUTION OF A GALACTIC DISK IN HIERARCHICAL MERGING OF COLD DARK MATTER HALOS

HIROHITO HAYASHI AND MASASHI CHIBA
Astronomical Institute, Tohoku University, Aoba-ku, Sendai 980-8578, Japan
Draft version November 21, 2018

ABSTRACT

We investigate the dynamical effects of dark matter subhalos on the structure and evolution of a galactic disk, using semi-analytic method that includes approximated and empirical relations as achieved in detailed numerical simulations of the cold dark matter model. We calculate the upper limit for the size of a galactic disk at a specific redshift z , based on the orbital properties of subhalos characterized by their pericentric distances from the center of a host halo. We find that this possibly largest size of a disk as determined by the smallest pericentric distances of subhalos shows the characteristic properties, which are basically in agreement with an observed galactic disk at low and high z . Namely, it is found that a massive disk can have a larger size than a less massive one, because of its stability against the destruction effect of subhalos. Also, with fixed mass, the size of a galactic disk at low z can be larger than that at high z , reflecting the orbital evolution of subhalos with respect to a host halo. These results suggest that the presence and structure of a galactic disk may be dynamically limited by the interaction with dark matter substructures, especially at high z .

Subject headings: cosmology: dark matter — galaxies: formation — galaxies: structure — galaxies: interactions

1. INTRODUCTION

The cold dark matter (CDM) model is now a standard theory for the structure formation of the universe. The model provides us with a basic theoretical framework for understanding the hierarchical clustering of dark matter, where large dark halos are assembled via merging and accretion of smaller halos. Indeed, the prediction of the CDM model is in excellent agreement with observations of large-scale structures (Tegmark et al. 2004). However, recent high-resolution N-body simulations based on the CDM model have highlighted that as a result of these merging processes, a large dark halo like that of the Milky Way contains numerous dark matter substructures or subhalos inside its virial radius, in contrast to the small number of known Milky Way satellites (Klypin et al. 1999; Moore et al. 1999). This so-called missing satellite problem remains unsolved yet, although various ideas are proposed to solve it based on, e.g., astrophysical baryonic processes such as UV feedback to suppress star formation and/or observational selection effects for faint satellite galaxies in the Milky Way (e.g., Bullock, Kravtsov & Weinberg 2000; Madau et al. 2008; Tollerud et al. 2008; Koposov et al. 2008; Koposov et al. 2009; Macciò et al. 2009).

If such dark matter subhalos indeed exist around a disk galaxy and some of these, especially massive ones, interact with a galactic disk in the course of their orbital motions, then the stellar component of a galactic disk can be made so thick due to dynamical heating that it no longer exists as a thin stellar disk like that of the Milky Way at the present epoch. This issue has been investigated by many researchers as a constraint on models of galaxy formation and evolution (e.g., Tóth & Ostriker 1992; Font et al. 2001; Ardi et al. 2003; Hayashi & Chiba 2006; Villalobos & Helmi 2008; Hopkins et al. 2008; Purcell et al. 2009). Hopkins et al. (2008) recently showed, based on the realistic (radial) orbits of subhalos as ob-

tained from cosmological simulations, that disk heating is less powerful than previously thought by Tóth & Ostriker (1992), which is based on the simple assumption of rigid satellites with circular orbits. To test what this result implies for satellite accretion with high mass, Purcell et al. (2009) made high-resolution numerical simulations for satellite-disk interactions and showed that in reality accretion events of mass ratio $\sim 1:10$ do not preserve thin disk components. Indeed, Stewart et al. (2008) demonstrated, also based on N-body simulations, that a majority ($\sim 70\%$) of galaxy-sized halos with mass $M = 10^{12}M_{\odot}$ at $z = 0$ have accreted at least one object with $M > 10^{11}M_{\odot}$ over the last 10 Gyr and $\sim 95\%$ have accreted an object with mass greater than Milky Way disk ($M > 5 \times 10^{10}M_{\odot}$). As these works suggest, a galactic disk is a fragile system, so that its dynamical evolution may be severely limited by these subhalos. In particular, the presence of a thin galactic disk at the present epoch implies the absence of the effect of subhalos within its size, which suggests in turn that the size of a galactic disk may be regulated by the orbital radii of subhalos. Therefore it is important to investigate the relation between the size evolution of a galactic disk and dynamics of subhalos within a host halo.

Several models for the structural evolution of a galactic disk have been studied (Mo, Mao & White 1998, hereafter MMW98; Bouwens & Silk 2002, hereafter BS02; Kampakoglou & Silk 2007). The evolution models can be divided into two alternative approaches, one is forward approach and the other is backward approach. The forward approach is based on the CDM model, where both collapsing dark matter and baryonic gas acquire the angular momentum through tidal force and mergers. When a gas component cools, condenses and forms stars, then the system's angular momentum halts the collapse, leading to the formation of a rotationally supported disk (Fall & Efstathiou 1980). Under the assumption that the frac-

tions of disk mass and angular momentum in the disk relative to the halo, together with the spin parameter of the halo, do not vary during this collapsing phase, Mo, Mao & White (1999) obtained the following relations for the scale length of an exponential stellar disk: $R_d \propto H(z)^{-1}$ at a fixed circular velocity or $R_d \propto H(z)^{-2/3}$ at a fixed halo mass, where $H(z)$ is a Hubble parameter at z . On the other hand, the backward approach is based on the detailed models of the properties of local disk galaxies, e.g., gaseous, stellar, and metallicity profiles, as well as current star formation rate (SFR) and age-metallicity relationship. This approach uses the local universe as a reference. Then the properties of a galactic disk at high z are derived on the basis of those at present time and backward calculation in time. Using the Milky Way as reference and assuming the continuous infall of metal-free gas from outside, BS02 provide the following size-redshift relation for a disk: $r(z)/r(0) = 1 - 0.27z$.

Observational studies of a galactic disk have also been put forward by several researchers. Using the Sloan Digital Sky Survey (SDSS), Shen et al. (2003) showed the local size-mass relation, where a galactic disk with large mass has a larger scale length than that with small mass. Based on the Galaxy Evolution from Morphology and SEDs (GEMS) survey, Barden et al. (2005) presented the size-mass relation up to $z \sim 1$. Also, using the Faint Infrared Extragalactic Survey (FIRES), Trujillo et al. (2004) measured the size-mass relation in the rest-frame optical up to $z \sim 2.5$. Trujillo et al. (2006) presented that at a given mass the mean size of a galactic disk was ~ 2 times smaller at $z \sim 2.5$ than that we see today, using the result of FIRES, GEMS, and SDSS.

It is worth noting that models in both forward and backward approaches are in good agreement with these observational results. However, there are a couple of unresolved issues in these models. In forward approach, the model assumes that a gas disk forms a stellar disk instantaneously at the epoch of a halo virialization, whereby only the evolution of a host halo is taken into account. In backward approach, the model does not include the merging history of a host halo. Thus in these models, the important dynamical effects of subhalos on the structural evolution of a galactic disk are unclear. In particular, since subhalos are able to destroy a galactic disk and the probability of such events is expected to be high, the previous models are yet insufficient to understand the evolution of a galactic disk. Therefore, it is of great importance to fully take into account the effect of subhalos on the evolution model of a galactic disk.

We remark here that this aspect of a disk evolution is automatically included in high-resolution gasdynamical simulations of a collapsing galaxy in the context of the CDM model. However, many of such simulation works have produced a disk which is too small compared with a galactic disk at present time (e.g., Navarro, Frenk & White 1995), most probably because the simulation results are largely affected by yet poorly understood physical processes, such as star formation and supernova feedback, that work below the resolution limit. Indeed, Governato et al. (2007) showed that their simulation taking into account improved feedback models along with high numerical resolution largely minimizes the issue of a too small simulated disk. Here, to avoid such complexity

in understanding the calculated results, we concentrate on the dynamical effect of subhalos on a galactic disk and adopt a semi-analytic method that includes approximated and empirical relations as achieved in detailed numerical simulations of the CDM model.

The outline of this paper is as follows. In §2 we describe our semi-analytical model that we use for the merging and accretion of dark matter halos. In §3 we present the examples of our semi-analytical model and the results for the disk evolution. We summarize and discuss the implications of the current results in §4.

2. MODEL

We describe here the properties of subhalos in a host dark halo, in particular the mass accretion history and the orbital evolution of subhalos after they enter the virial radius of a host halo. For our current work, we adopt the semi-analytic model developed by Zentner & Bullock (2003), hereafter ZB03, with some modification as explained below. In the followings, we adopt the standard set of cosmological parameters: the density parameter at present $\Omega_{m0} = 0.3$, cosmological constant at present $\Lambda = 0.7$, Hubble constant $H_0 = 100h \text{ km s}^{-1} \text{ Mpc}^{-1}$ with $h = 0.72$, baryon fraction at present $\Omega_B h^2 = 0.02$, and rms density variation averaged over $8h^{-1} \text{ Mpc}$ as $\sigma_8 = 0.95$.

2.1. The ZB03 Model

2.1.1. Construction of Merger Trees

Following ZB03, we track the mass accretion history of a host halo using the extended Press-Schechter (EPS) theory (Bond et al. 1991; Lacey & Cole 1993, hereafter LC93) and adopt the merger tree algorithm proposed by Somerville & Kollat (1999, hereafter SK99). Using this method, we generate a list of the masses and accretion redshifts of all subhalos that have merged to form a host halo of a given mass at a given redshift. In the EPS formalism, the linear density field $\delta(M)$ as a function of the smoothing mass M is regarded as a random Gaussian field, which is specified by the mass variance $S(M)$. To derive this, we consider a density field smoothed with a spherical top-hat function with a radius R . Also, according to the spherical collapse model, the density field collapses and forms a virialized object at z once the density field δ exceeds $\omega = \delta_{\text{crit}}(z) \simeq 1.68$ (see LC93). Then, denoting $\Delta S = S(M) - S(M + \Delta M)$ and $\delta\omega = \omega(t) - \omega(t + \Delta t)$, the probability that a halo having mass M at time t has accreted the mass corresponding to a step of ΔS in a time step associated with $\delta\omega$ is given as

$$P(\Delta S, \delta\omega)d(\Delta S) = \frac{\delta\omega}{\sqrt{2\pi}\Delta S^{3/2}} \exp\left[-\frac{(\delta\omega)^2}{2\Delta S}\right]d(\Delta S). \quad (1)$$

Following SK99, we generate merger trees by starting the redshift $z = 0$ at which we consider the final halo and step backward in time. To reproduce the prediction of the conditional mass function of the EPS model, we must choose the appropriate time step. In this model we choose the time step given by Taylor & Babul (2004), $\delta\omega = [0.2 \log_{10}(M/M_{\text{min}}) + 0.1]\delta\omega_0$, where M_{min} is a resolution limit mass and $\omega_0 = \sqrt{(dS/dM)|_{M_{\text{min}}}}$. At each timestep we take a mass $S(M_p) = S(M) + \Delta S$ from

the probability equation (1). We treat events with $M_p < M_{\min}$ as accreted mass and retain all information about mergers with $M_p \geq M_{\min}$. In this way, we generate the list of progenitor masses and accretion redshifts at each time step. This process continues until the masses of all progenitors are less than M_{\min} . At each time step we identify the most massive progenitor with the host halo and all less massive progenitor with accreted subhalos.

We note here that the recent work by Zhang, Fakhouri & Ma (2008) showed cautionary remarks in the use of the SK99 model, which overestimates the abundances of small progenitor halos as large as a factor of about 2 compared to the prediction of the EPS formalism. Although a quantitative estimation for the effect of adopting different Monte Carlo algorithms from SK99 is beyond the scope of this work, our results based on the distribution of pericentric orbital radii of subhalos, as detailed later, would not be sensitive to their precise abundances at each redshift.

2.1.2. Density Distribution of Halos

The spherical collapse model provides the density of a virialized region for a dark halo. The density of a virialized halo is given as $\rho_{\text{vir}} = \rho_m \Delta_{\text{vir}}$, where ρ_m is the mean matter density of the universe. For Δ_{vir} , we use the fitting function provided by Bryan & Norman (1998), where for our cosmological parameters, $\Delta_{\text{vir}} \approx 370$ at $z = 0$ and $\Delta_{\text{vir}} \approx 179$ at high z . Then the virial radius of a virialized halo with mass M_{vir} at z is

$$R_{\text{vir}} = (3M_{\text{vir}}/4\pi\Delta_{\text{vir}}\rho_m)^{1/3} \quad (2)$$

and the circular velocity at the virial radius, so-called virial velocity, is $V_{\text{vir}} = (GM_{\text{vir}}/R_{\text{vir}})^{1/2}$.

Recent numerical simulations discover the several analytical density profile of a dark halo (Navarro, Frenk & White 1997, hereafter NFW; Moore et al. 1998). We choose the NFW profile as the density profile of all halos:

$$\rho(r) = \frac{\rho_s}{(r/r_s)(1+r/r_s)^2}, \quad (3)$$

where the maximum circular velocity is achieved at $r_{\text{max}} \simeq 2.16r_s$. The NFW profile is characterized by the concentration parameter $c_{\text{vir}} = R_{\text{vir}}/r_s$. Numerical simulations suggest several analytical functions with the mass of a halo and a redshift, $c_{\text{vir}} = c_{\text{vir}}(M, z)$ (NFW; Bullock et al. 2001, hereafter B01; Eke, Navarro & Steinmetz 2001; Macciò, Dutton & van den Bosch 2008). In our model, we use the model of B01 for the concentration parameter of a dark matter halo having mass M_{vir} at redshift z , which has collapsed at redshift z_c : $c_{\text{vir}}(M, z) = K(1+z_c)/(1+z)$, where B01 suggest $K = 4$ since this agrees well with the result of their Λ CDM simulations. This expression for $c_{\text{vir}}(M, z)$ indicates that massive halos are less concentrated than less massive halos and that a halo at low z is more concentrated than that at high z . Since $R_{\text{vir}} \propto \Delta_{\text{vir}}^{1/3}(1+z)$, an inner radius r_s is almost constant at all z .

2.1.3. Orbital Evolution of Subhalos

We track the orbital evolution of all accreted subhalos, taking into account the dynamical friction and tidal mass loss while orbiting in a host halo. Through these processes, subhalos eventually sink to the center of the

host halo (termed ‘‘central merged’’ in ZB03), or lose the most of the mass (‘‘tidal disrupted’’), or keep the distinct structure from their accretion epoch to the present. We model these processes based on the ZB03 formalism.

We define that a subhalo has a mass M_{sat} and outer radius R_{sat} at the accretion redshift of z_{acc} obtained by our merger tree, where R_{sat} is given by R_{vir} [equation (2)]. The concentration parameter of a subhalo is calculated from the median value as given by M_{sat} and z_{acc} at the accretion. Notice that R_{sat} and M_{sat} are varied due to mass loss while orbiting within a host halo. We update the mass and concentration parameter of the host halo at each accretion event and continue to fix its density structure of the host halo while each orbit is integrated. In order to track the orbit of each subhalo, we assume the potential of the host halo to be spherically symmetric and static, so the orbit of a subhalo depends only on the radial distance from the center of the host halo.

When it accretes onto the host halo, we assume that each subhalo has an initial orbital energy, which is consistent with the result of detailed N-body simulations by, e.g., Klypin et al. (1999). Namely, as described in ZB03, each subhalo has an initial orbital energy equal to the energy of a circular orbit at the radius $R_{\text{circ}} = \eta R_{\text{vir}}$, where R_{vir} is the virial radius at the accretion and η is drawn randomly from a uniform distribution on the interval $[0.4, 0.75]$. In this way, we define the absolute velocity of a subhalo at the accretion. Next we consider the velocity vector of a subhalo. We define the initial angular momentum of a subhalo at the accretion as $J = \epsilon J_{\text{circ}}$, where J_{circ} is the angular momentum for a circular orbit of the same energy and ϵ is a parameter, so-called ‘‘orbital circularity’’ (LC93). Recent numerical simulations show that this orbital circularity is well fitted by beta distribution (Zentner et al. 2005):

$$\frac{df(\epsilon)}{d\epsilon} = \frac{\Gamma(2a)}{\Gamma^2(a)} \epsilon^{a-1} (1-\epsilon)^{a-1}, \quad (4)$$

where $a = 2.22$ provides a good fit to their Λ CDM simulation results with the mean $\langle \epsilon \rangle = 1/2$ and the dispersion $\sigma(\epsilon) = 1/2(2a+1)^{1/2}$. This form of the orbital circularity is also in agreement with the results obtained from cosmological simulations by Benson (2005) and Khochfar & Burkert (2006). We define that the initial radial position of a subhalo at the accretion is R_{circ} and its orbit is given by $dR/dt < 0$ in order to be initially infalling. For the calculation of its orbital decay by dynamical friction, we assume a subhalo as being represented by a point mass in the gravitational potential of the host halo. We use the standard Chandrasekhar formula (Chandrasekhar 1943) for the evaluation of the frictional force, following the method shown in ZB03.

The mass of a subhalo is stripped by the tidal force while orbiting in the potential of the host halo. This process is approximately modeled as follows. First, the instantaneous tidal radius r_t of the subhalo at each point along its orbit is calculated by the equation, in the limit that a subhalo is much smaller than a host halo, as (e.g., King 1962)

$$r_t^3 \simeq \frac{M_{\text{sat}}(< r_t)/M_{\text{host}}(< r)}{2 + \omega^2 r^3 / GM_{\text{host}}(< r) - \partial \ln M_{\text{host}}(< r) / \partial \ln r} r^3, \quad (5)$$

where r is the radial position of a subhalo in the host halo, $M_{\text{host}}(< r)$ is the mass of the host halo within

r , $M_{\text{sat}}(< r_t)$ is the mass of the subhalo within r_t , ω is the instantaneous angular speed of the orbiting subhalo $\omega = L/r^2$, and L is the angular momentum of the subhalo. The process of the mass loss occurring outside r_t is calculated following Taylor & Babul (2001): we divide the orbit of the subhalo into discrete time steps of size $\delta t \ll T$, where T is the orbital time scale $T = 2\pi/\omega$, then at each time step, we remove the mass $\delta m = M_{\text{sat}}(> r_t)(\delta t/T)$, where $M_{\text{sat}}(> r_t)$ is the mass of the subhalo outside r_t . While a subhalo loses mass due to tidal force, its density profile is assumed to remain unchanged within its outer radius R_{sat} , which is now defined as the radius within which the bound mass is contained in the form of an NFW profile. We continue to fix the scale radius of the subhalo, r_s^{sat} , at the value calculated at the epoch of the accretion.

Finally, we define whether a subhalo is tidally disrupted, centrally merged, or survived, following the criteria given in ZB03. We first set $r_{\text{max}}^{\text{sat}} \simeq 2.16r_s^{\text{sat}}$ as the radius at which the initial circular-velocity profile of a subhalo reaches its maximum, and its mass $M_{\text{sat}}(< r_{\text{max}}^{\text{sat}})$ within $r_{\text{max}}^{\text{sat}}$. We consider a subhalo to be ‘‘tidally disrupted’’ if its mass becomes less than $M_{\text{sat}}(< r_{\text{max}}^{\text{sat}})$. A subhalo is ‘‘centrally merged’’ with the host halo if its radial position, r , becomes smaller than $r_{\text{max}}^{\text{sat}}$. Also, the mass lost by tidal force modifies the circular-velocity profile of subhalos. To account for this effect, following ZB03, we determine whether or not the tidal radius of each surviving subhalo has ever been less than $r_{\text{max}}^{\text{sat}}$. If the subhalo experienced so, we change the maximum circular velocity of the subhalo by $V_{\text{max}}^{\text{final}} = (M_{\text{sat}}^{\text{final}}/M_{\text{sat}}^{\text{initial}})^{1/3}V_{\text{max}}^{\text{initial}}$, where $V_{\text{max}}^{\text{initial}}$ is the maximum circular velocity of the initially defined subhalo, $M_{\text{sat}}^{\text{final}}$ is its final mass, and $M_{\text{sat}}^{\text{initial}}$ is its initial mass at the accretion.

2.2. Model Checks

Following ZB03, we have calculated the three examples for the orbits of subhalos. For all of these cases, we adopt the same initial condition of $\epsilon = 0.5$ and $\eta = 0.5$ for each subhalo’s orbit, with the concentration and the mass of the host halo being $c_{\text{vir}} = 6$ and $M_{\text{host}} = 5 \times 10^{11} M_{\odot}$, respectively. The other parameters of the subhalos are given as follows: $M_{\text{sat}}^0 = 10^8 M_{\odot}$, $c_{\text{vir}} = 15$; $M_{\text{sat}}^0 = 10^8 M_{\odot}$, $c_{\text{vir}} = 7.5$; $M_{\text{sat}}^0 = 5 \times 10^9 M_{\odot}$, $c_{\text{vir}} = 15$. The results are shown in Figure 1, where the upper panel shows the evolution of radial positions of the subhalos and the lower panel shows the evolution of their masses of the subhalos. We set the start of calculation to be at 8 Gyr ago, which is $z \simeq 1.14$ for our cosmology. The plots in this figure are in excellent agreement with Figure 3 in ZB03, indicating that our model successfully reproduces their results.

We show, in Figure 2, the cumulative velocity function to demonstrate the statistical properties of our model. The plots correspond to an ensemble mean of 200 host halos with mass $1.4 \times 10^{12} M_{\odot}$ at $z = 0$, where these host halo systems have the maximum circular velocity $V_{\text{max}} \simeq 188 \text{ km s}^{-1}$, the virial radius $R_{\text{host}} \simeq 285 \text{ kpc}$, and the concentration parameter $c_{\text{vir}} \simeq 13.4$. We use $M_{\text{min}} = 10^5 M_{\odot}$. It is found that the cumulative velocity function of the survived subhalos until $z = 0$ is in good agreement with Figure 4 of ZB03 and also the result of

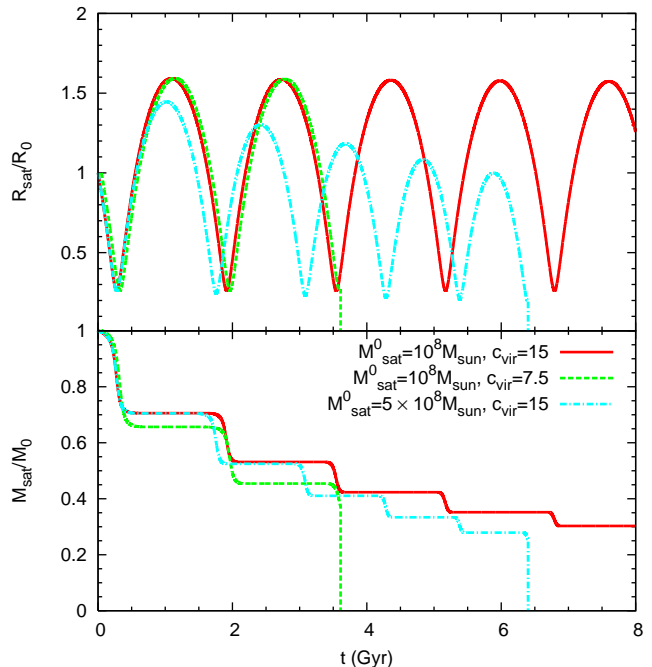


FIG. 1.— Orbital evolution for three sets of the subhalo parameters: Initially at $t = 0$, $M_{\text{sat}}^0 = 10^8 M_{\odot}$, $c_{\text{vir}} = 15$ (solid line); $M_{\text{sat}}^0 = 10^8 M_{\odot}$, $c_{\text{vir}} = 7.5$ (dashed line); $M_{\text{sat}}^0 = 5 \times 10^9 M_{\odot}$, $c_{\text{vir}} = 15$ (dash-dotted line). The host halo is given by $c_{\text{vir}} = 6$ and $M_{\text{host}} = 5 \times 10^{11} M_{\odot}$. The top panel shows the radial evolution in units of the initial radius as a function of time. The bottom panel shows the mass evolution in units of the initial mass as a function of time, where the vertical lines correspond to the end point when the subhalos are destroyed.

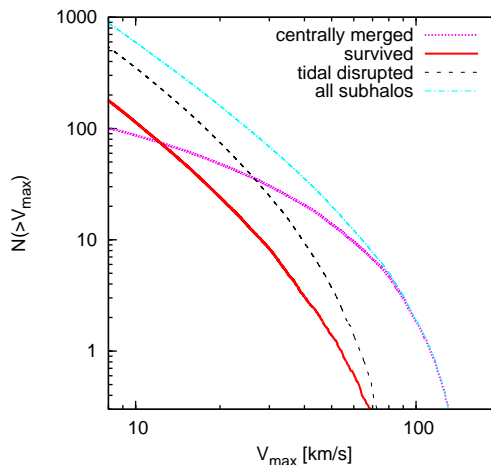


FIG. 2.— Cumulative velocity function of the survived and destroyed subhalos for the host mass $M_{\text{host}} = 1.4 \times 10^{14} M_{\odot}$ at $z = 0$. These plots are an ensemble mean of 200 host halo systems. Each line is for the survived subhalos until the present epoch (thick solid line), tidally destroyed ones (dashed line), central-merged ones (thick dotted line), and all of the accreted subhalos as obtained from the merging history (dash-dotted line), respectively.

the numerical simulation by Klypin et al. (1999).

2.3. Method for Calculating Likely Disk Sizes

A host halo contains numerous subhalos, among which there exist several very massive ones with mass of $M \sim 10^{10} M_{\odot}$. In this study, we assume that when such a massive subhalo having a comparable mass to a galactic

stellar disk of $M \sim 10^{10} M_{\odot}$ interacts with each other, then a stellar disk is made so thick due to dynamical heating that it no longer exists as a thin stellar disk like that of the Milky Way at the present epoch (e.g., Hayashi & Chiba 2006; Villalobos & Helmi 2008). More specifically, we assume that if a subhalo having this large mass interacts with a galactic disk at any radial positions, then the latter is supposed to be destroyed by a subhalo. To account for this process in our model, we calculate, for the redshift interval of z to $z + dz$, the minimum of pericentric radii r_{\min} for subhalos' orbital motions, where their mass is larger than a supposed mass of a galactic disk (M_{th}). We then suppose that this minimum radius provides the upper limit for the radius of a galactic disk which can exist at z . It is thus postulated that any galactic disk having a size larger than this minimum of subhalos' pericentric radii will be destroyed by dynamical interaction with subhalos. In other words, the size of a galactic disk at z is limited by the orbits of massive subhalos in the redshift interval of z to $z + dz$.

We note that in the actual calculation of merger trees, there are only a few subhalos with mass $M > M_{\text{th}}$ from z to $z + dz$, which makes it difficult to estimate the minimum of pericentric radii in the interval z to $z + dz$ in a statistically significant manner. Instead, we first consider the cumulative distribution from z to $z = 0$, for the minimum of pericentric radii for subhalos with $M > M_{\text{th}}$. We then convert this cumulative form with respect to z into the differential form from z to $z + dz$. Notice that in this calculation we exclude the subhalos which end up with ‘‘centrally merged’’. Such subhalos sink to the center of the host halo, which results in major mergers with a galactic disk. Therefore, by excluding such subhalos, we can examine a dynamically quiet disk system that does not experience any major-merger events, thereby having a possibility to exist as a galactic disk.

3. RESULTS

3.1. Distribution of Pericentric Radii of Subhalos

Here we show the fiducial case of a host halo with $M_{\text{host}} = 1.4 \times 10^{12} M_{\odot}$ at $z = 0$ and the minimum mass of merger tree is $M_{\min} = 10^5 M_{\odot}$. Figure 3 - 5 show the histogram of the minimum of pericentric radii for orbiting subhalos with $M > M_{\text{th}}$ from z to $z = 0$. In these figures, we vary z from 0.3 to 1.8. Figure 3, 4, and 5 show, respectively, the cases of $M_{\text{th}} = 10^{10} M_{\odot}$, $6 \times 10^9 M_{\odot}$, and $3 \times 10^9 M_{\odot}$, based on 200 merger trees. It is found that at fixed M_{th} , r_{\min} at higher z is smaller than that at lower z . This can be explained as follows. At high z the virial radius of a host halo is small as suggested from equation (2). Also the orbital time of subhalos which accreted at higher z is longer than those accreted at lower z . Thus the orbits of subhalos with longer orbital time decay more to inner radii since dynamical friction affects these subhalos during a longer time, thereby yielding smaller r_{\min} . On the other hand, at fixed z , r_{\min} for larger M_{th} is larger than that for smaller M_{th} . This may be because the accretion of massive subhalos occur at preferentially low z , compared with less massive ones.

Figure 6 shows the average of these histograms (plus, cross, and asterisk). The lines denote the fitting functions in terms of the least-squares method (without employing a dispersion-weighted fitting), which are given as $22(1+z)^{-0.54}$ for $M_{\text{th}} = 10^{10} M_{\odot}$, $17(1+z)^{-0.56}$

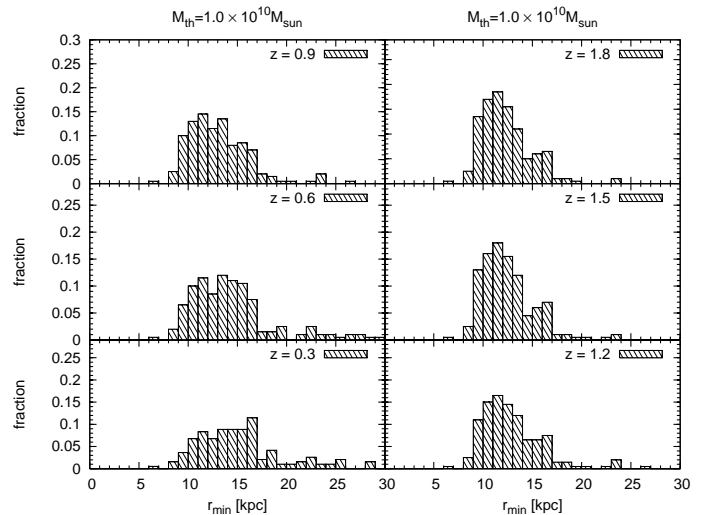


FIG. 3.— The histogram of the minimum of pericentric radii for orbiting subhalos with the mass larger than $M_{\text{th}} = 10^{10} M_{\odot}$ from the given redshift z to $z = 0$ in each merger tree. In the upper right corner this z is depicted. We exclude the subhalos which end up with centrally merged. The grid of the histogram is 1 kpc. All the panels are based on the 200 merger trees.

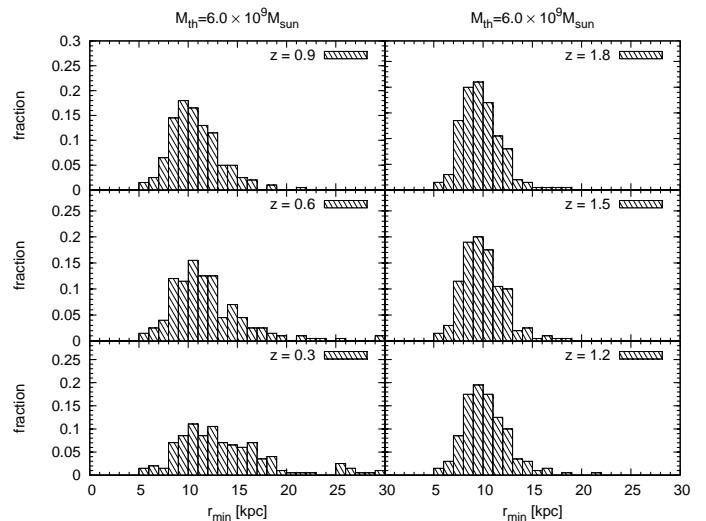


FIG. 4.— The same as Figure 3 but for $M_{\text{th}} = 6 \times 10^9 M_{\odot}$.

for $M_{\text{th}} = 6 \times 10^9 M_{\odot}$, and $12(1+z)^{-0.53}$ for $M_{\text{th}} = 3 \times 10^9 M_{\odot}$. If a dispersion is used so that a fitting is weighted in favor of a low dispersion, we obtain somewhat shallower fitting curves: $19(1+z)^{-0.38}$, $13(1+z)^{-0.27}$, and $11(1+z)^{-0.42}$, respectively. These plots show clearly that at fixed M_{th} , r_{\min} at high z is smaller than that at low z and at fixed z , r_{\min} with massive M_{th} is larger than that with less massive one.

In addition to these cases with a threshold subhalo mass of $M_{\text{th}} \leq 10^{10} M_{\odot}$, we additionally consider much more massive cases, i.e., $M_{\text{th}} = 5 \times 10^{10} M_{\odot}$ and $10^{11} M_{\odot}$ in view of recent studies (Stewart et al. 2008; Purcell et al. 2009) showing that such massive subhalos are most crucial in the survival of a thin disk. In Figure 6, open and filled squares show the cases of these threshold masses, respectively. It is found that such massive subhalos, which do not end up with the cate-

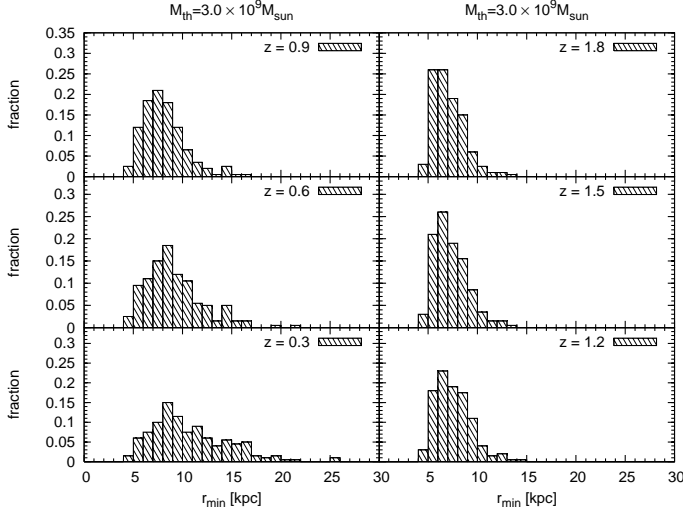


FIG. 5.— The same as Figure 3 but for $M_{\text{th}} = 3 \times 10^9 M_{\odot}$.

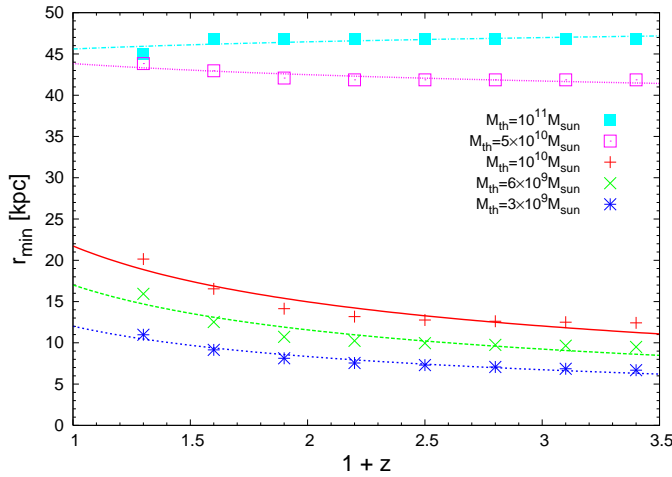


FIG. 6.— Ensemble mean of the minimum of pericentric radii for orbiting subhalos with the mass larger than $M_{\text{th}} = 10^{10} M_{\odot}$ (plus), $6 \times 10^9 M_{\odot}$ (cross), and $3 \times 10^9 M_{\odot}$ (asterisk) from redshift z to $z = 0$. Also, shown are the additional two cases with more massive subhalos, $M_{\text{th}} = 10^{11} M_{\odot}$ (filled square) and $5 \times 10^{10} M_{\odot}$ (open square). All the plots are based on the result of 200 merger trees. All the lines are the results of the least-squares fitting to these plots for the ensemble mean.

gory of centrally merged ones, remain at large orbital distances of > 40 kpc and that the distribution of their pericentric distances stays nearly constant: the fitting functions are given as $44(1+z)^{-0.05}$ and $46(1+z)^{+0.03}$ for $M_{\text{th}} = 5 \times 10^{10} M_{\odot}$ and $10^{11} M_{\odot}$, respectively, for both with and without using a dispersion in the fitting procedure. Thus, a disk which is exempt from the central merging of such massive subhalos is likely able to have a large radius, unless the effects of less massive ones are significant.

To derive the distribution from z to $z + dz$, we convert these fitting functions into differential forms as follows. We define $N(z, R_{\text{size}}, M_{\text{disk}})$ as the distribution function of galactic disks with the size, R_{size} , and mass, M_{disk} , at z . Considering the average of the size of galactic disks

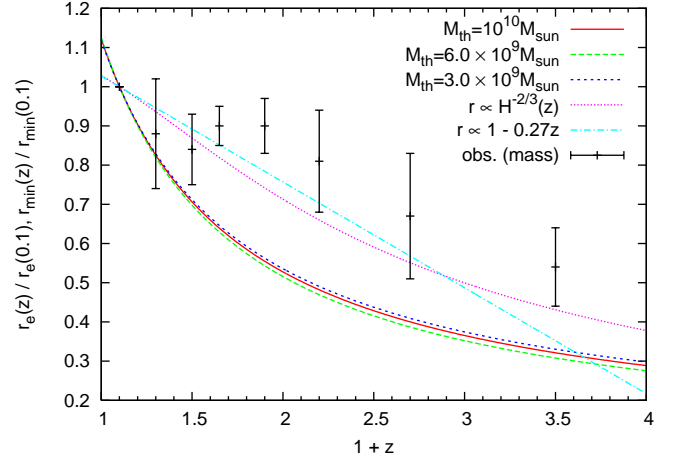


FIG. 7.— Redshift dependence of disk-size evolution in various disk models and observed disks, where comparison is made by normalizing a disk size to be 1 at $z = 0.1$. Solid, long-dashed, and short-dashed lines denote the fitting results (without considering the dispersion) to the average of the minimum pericentric radius r_{min} in subhalos with mass which is larger than $M_{\text{th}} = 10^{10} M_{\odot}$, $6 \times 10^9 M_{\odot}$, and $3 \times 10^9 M_{\odot}$, respectively, from z to $z + dz$. Also shown are other model predictions: dotted line is the expected evolution of disk scale length from Mo et al. (1999) $r_e(z)/r_e(0.1) \propto H^{-2/3}(z)$, and dash-dotted line is the expected evolution of disk scale length from BS02 $r_e(z)/r_e(0.1) \propto 1 - 0.27z$, where r_e is the effective radius. The points denote the evolution of an average disk scale length from observational result (Trujillo et al. 2006), $r_e(z)/r_e(0.1)$.

from the redshift z to $z = 0$, then we can write this as,

$$\langle R_{\text{size}} \rangle = \frac{\int_0^{\infty} R'_{\text{size}} \int_z^0 N(z', R'_{\text{size}}, M_{\text{disk}}) dz' R'_{\text{size}}}{\int_0^{\infty} \int_z^0 N(z', R'_{\text{size}}, M_{\text{disk}}) dz' dR'_{\text{size}}} \quad (6)$$

Assuming that all disks are destroyed when subhalos with mass larger than the threshold mass M_{th} (comparable to a disk mass) interact with anywhere inside a galactic disk, $\langle R_{\text{size}} \rangle$ agrees with the minimum of pericentric radius for orbiting subhalos with mass larger than M_{th} from the redshift z to $z = 0$. We define the distribution of galactic disks with mass smaller than M_{disk} from z to $z + dz$ as $\overline{R_{\text{size}}}$. We can write this as

$$\overline{R_{\text{size}}} = \frac{\int_0^{\infty} R'_{\text{size}} N(z, R'_{\text{size}}, M_{\text{disk}}) dR'_{\text{size}}}{\int_0^{\infty} N(z, R'_{\text{size}}, M_{\text{disk}}) dR'_{\text{size}}} \quad (7)$$

With normalization $\int_0^{\infty} N(z, R'_{\text{size}}, M_{\text{disk}}) dR'_{\text{size}} = 1$, we obtain

$$\langle R_{\text{size}} \rangle = \frac{1}{z} \int_0^z dz' \overline{R_{\text{size}}}(z'). \quad (8)$$

Assuming $\langle R_{\text{size}} \rangle = \alpha(1+z)^{\beta}$ and employing differentiation, we obtain

$$\overline{R_{\text{size}}}(z) = \alpha(1+z)^{\beta-1} [1 + (1+\beta)z]. \quad (9)$$

In this way, we can convert the cumulative function over $[0, z]$ into the differential function over $[z, z + dz]$.

Figure 7 shows these differential functions normalized at $z = 0.1$, so that redshift dependence of size evolution is highlighted. It is evident that there is no significant difference in redshift dependence between our models with different mass thresholds M_{th} . We also plot the prediction of the existing disk evolution models: Mo, Mao &

White (1999) model of $r_e(z)/r_e(0.1) \propto H^{-2/3}(z)$ (dotted line) and BS02 model of $r_e(z)/r_e(0.1) \propto 1 - 0.27z$ (dash-dotted line), where r_e is the effective radius. Also shown (points with error bars) is the evolution of average disk scale length from observational results (Trujillo et al. 2006). It follows that the redshift dependence of all the characteristic sizes is basically similar to each other, especially at $z \gtrsim 1$.

3.2. Comparison with Observed Disk Sizes

Our interest in this work is to elucidate whether a galactic disk survives in the CDM model. For this purpose, we need to estimate the likely outer edge of an observed disk, which generally has an exponential light distribution. For a class of disk galaxies, this light distribution does not extend to an arbitrarily large radius, but is radially truncated at the outer part. This radius is a so-called truncation radius, which can be regarded as the outer edge of the disk. Observations of nearby disk galaxies indicate that this truncation radius is related to the disk scale length as $R_{\text{break}} \approx 2R_d - 4R_d$ (e.g. Kregel et al. 2002). In contrast, at high z few observations are available for the information of a truncation radius. We simply assume the relation $R_{\text{break}} = 3.5R_d$ at current epoch for such remote disk galaxies.

We consider the Milky Way-type disk with mass $10^{10}M_\odot$ and the scale length $R_d = 4$ kpc for the present experiment, to obtain the evolution of the disk's outer edge. In Figure 8, the points show the redshift evolution of a supposed disk size at fixed mass as derived from an observed disk scale length. Notice that we assume r_e is equal to R_d , since the effective radius is related to the scale length by a simple function. It follows that at low z the points are well below our theoretical upper limits, thereby suggesting that observed galactic disks at low z can survive in the CDM model. On the other hand, at high z there is a possibility that some of galactic disks may be destroyed by dynamical effects of subhalos, yielding some slight disagreement with observations. This possibility can be precluded by other effects occurred in a disk. For instance, when a galactic disk contains the large amount of cold interstellar gas, such gas which is unaffected by subhalos can reduce the thickness of a galactic disk. Also, at the truncation radius the mass density of a galactic disk are low enough that the effect of subhalos on a disk structure is minor.

4. DISCUSSION AND CONCLUDING REMARKS

We have investigated the dynamical effect of subhalos on the size evolution of a galactic disk, based on a semi-analytic method that includes approximated and empirical relations for the evolution of subhalos as obtained in detailed numerical simulations of the CDM model. This is motivated by our previous work (Hayashi & Chiba 2006) that subhalos are able to induce the dynamical heating and tidal destruction of a galactic disk, thereby affecting the distribution of the size of a disk which does not suffer from the interaction with subhalos; such a disk ought to be smaller than the minimum of pericentric orbital radii of subhalos. We have found that the upper limit for the size of a galactic disk with large mass is larger than that with small mass. Also, with fixed mass, the upper limit for the size of a galactic disk at low z is larger than that at high z .

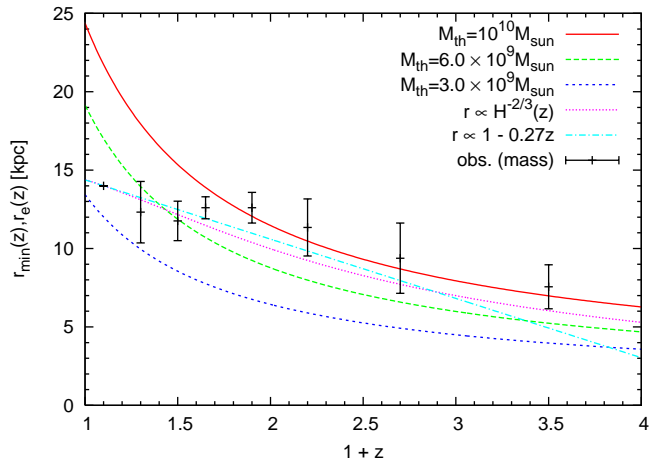


FIG. 8.— The same as Figure 7 but without being normalized. We assume a Milky Way type disk, where $r_e(0.1) = 4$ kpc and the size of a disk is $3.5r_e$.

Stellar-population analyses of present-day galaxies have revealed the so-called 'downsizing' evolution, where the stars in more massive galaxies tend to have formed earlier and over a shorter time-span (Thomas et al. 2005; MacArthur et al. 2004). On the other hand, in the CDM model halos are formed hierarchically in a bottom-up manner, contrary to the downsizing evolution. In view of this general downsizing evolution of galaxies, our result that a galactic disk with larger size and mass is available only at lower z may conflict with observations. However, it is noted that this evolution of a disk is limited by the pericentric orbital radius of subhalos, i.e., a disk which has never been affected by subhalos, whereas a galactic disk having initially a large radius can indeed be dynamically heated and/or tidally destroyed by subhalos. Even after such a destruction incident of a thin stellar disk, residual gas or infalling fresh gas allows to form a new disk component. Indeed according to recent numerical simulations, infalling subhalos do not fully destroy a galactic disk, where some fraction of the thin disk component are survived (Kazantzidis et al. 2008; Villalobos & Helmi 2008). We thus regard that old stellar components in massive disk galaxies may be the relic of a first-existing galactic disk. In particular, recent numerical simulations have demonstrated that a thick disk can be formed by the dynamical interaction between such a first-existing disk and subhalos (Hayashi & Chiba 2006; Kazantzidis et al. 2008; Villalobos & Helmi 2008).

Several models have been proposed for the evolution of a disk scale length (e.g., MMW98; BS02). However, such models do not explicitly take into account the finite extent of a galactic disk. For instance, the MMW98 model assumes that stars form from gas instantaneously, while maintaining an exponential density profile of a disk. Since an exponential disk does not have an outer limit in its profile, this model cannot provide the size evolution of a galactic disk. On the other hand, the BS02 model adopts the present state of a disk galaxy as an initial condition for its backward approach in time. This model also assumes an exponential stellar disk at present, so it is unclear how the disk size evolves; we need to take into account explicitly the size evolution of a disk in its model for the formation of an exponential density profile.

As such a model, we consider a so-called viscous disk model (Lin & Pringle 1987; Yoshii & Sommer-Larsen 1989). This model shows that the exponential distribution of stars in a galactic disk is a natural product of angular momentum redistribution caused by viscosity. Yoshii & Sommer-Larsen (1989) found that if the condition that star formation time scale being comparable to viscous time scale is maintained, then the final stellar distribution shows an exponential profile irrespective of the specific form of the initial gas profile. However, since stars are assumed to form continuously as long as gas is still remained, where fresh gas is always replenished by infalling gas, it is evident in this model that no outer limit comes out in a galactic disk. We thus need to consider, for instance, the star formation threshold in this model, to obtain the size evolution of a galactic disk, where stars are formed when gas density is beyond some threshold value. Such a threshold in gas density may be defined by a so-called Toomre criterion for gravitational instability of an axisymmetric disk and/or some external feedback such as a UV background radiation, although an explicit account of these processes is yet to be explored in a viscous disk model.

It is worth noting that in our models presented here, a couple of other effects, e.g., gas-dynamical response of a disk and tidal force of a disk on subhalos are ignored. When we consider cold gas components in a disk, the stronger binding energy of such a disk than that without gas may be less affected by subhalos. Also, the tidal force of a disk on subhalos may make the mass loss of subhalos more significant. Both of these effects help the survival of a galactic disk. If we assume that the orbital circularity of subhalos is more tangential than that adopted here, the number of subhalos having nearly circular orbits becomes larger. Then subhalos can be more easily survived at larger orbital radii, so the size of a galactic disk limited by such subhalos may be larger. This

therefore suggests that it is essential to understand the realistic dynamical properties of subhalos, based on the CDM model, in order to set tighter constraints on the evolution of a disk galaxy like the Milky Way.

We conclude that subhalos tightly regulate the structure and evolution of a galactic disk. The effects of massive subhalos on a galactic disk are significant compared to less massive ones, so it is important to consider the dynamics and properties of such subhalos. Since at high z subhalos can sink to the central region of a host halo, the dynamical effects of subhalos on a galactic disk is more efficient at high z than at low z . Then, a galactic disk at present might experience the interaction with subhalos one or more times during its evolutionary process, especially at high z . We postulate that a thick disk is a relic of a pre-existing galactic disk after these interaction events.

It is also important to construct the new formation model of a galactic disk taking into account its size evolution and dynamical effects of subhalos, so that one can directly compare the model results with observed disks at high z . In this respect, it is useful to carry out high-resolution hydrodynamical simulations and predict detailed properties of galactic disks at high z . Furthermore, more detailed observations of extragalactic thick disks, in particular their kinematics, are needed to find the evidence for the interaction between subhalos and a galactic disk (e.g., Herrmann, Ciardullo, & Sigurdsson 2009).

The authors are grateful to the anonymous referee for useful comments that helped improve the manuscript. This work has been supported in part by a Grant-in-Aid for Scientific Research (20340039) of the Ministry of Education, Culture, Sports, Science and Technology in Japan.

REFERENCES

- Ardi, E., Tsuchiya, T., & Burkert, A. 2003, *ApJ*, 596, 204
 Barden, M., et al. 2005, *ApJ*, 635, 959
 Benson, A. J. 2005, *MNRAS*, 358, 551
 Bond, J. R., Cole, S., Efstathiou, G., & Kaiser, N. 1991, *ApJ*, 379
 Bouwens, R. J., & Silk, J. 2002, *ApJ*, 568, 522 (BS02)
 Bullock, J. S., Kravtsov, A. V., & Weinberg, D. H. 2000, *ApJ*, 539, 517
 Bullock, J. S., Kolatt, T. S., Sigad, Y., Somerville, R. S., Kravtsov, A. V., Klypin, A. A., Primack, J. R., & Dekel, A. 2001, *MNRAS*, 321, 559 (B01)
 Bryan, G. L., & Norman, M. L. 1998, *ApJ*, 495, 80
 Chandrasekhar, S. 1943, *ApJ*, 97, 255
 Eke, V. R., Navarro, J. F., & Steinmetz, M. 2001, *ApJ*, 554, 114
 Fall, S. M., & Efstathiou, G. 1980, *MNRAS*, 193, 189
 Font, A. S., Navarro, J. F., Stadel, J., & Quinn, T. 2001, *ApJ*, 563, L1
 Governato, F., et al. 2007, *MNRAS*, 374, 1479
 Hayashi, H., & Chiba, M. 2006, *PASJ*, 58, 835
 Herrmann, K. A., Ciardullo, R., & Sigurdsson, S. 2009, *ApJ*, 693, L19
 Hopkins, P. F., Hernquist, L., Cox, T. J., Younger, J. D., & Besla, G. 2008, *ApJ*, 688, 757
 Kampakoglou, M., & Silk, J. 2007, *MNRAS*, 380, 646
 Kazantzidis, S., Bullock, J. S., Zentner, A. R., Kravtsov, A. V., & Moustakas, L. A. 2008, *ApJ*, 688, 254
 Khochfar, S., & Burkert, A. 2006, *A&A*, 445, 403
 King, I. 1962, *AJ*, 67, 471
 Klypin, A., Kravtsov, A. V., Valenzuela, O., & Prada, F. 1999, *ApJ*, 522, 82
 Kposov, S., et al. 2008, *ApJ*, 686, 279
 Kposov, S., et al. 2009, *ApJ*, 696, 2179
 Kregel, M., van der Kruit, P. C., & de Grijs, R. 2002, *MNRAS*, 334, 646
 Lacey, C. G., & Cole, S. M. 1993, *MNRAS*, 262, 626 (LC93)
 Lin, D. N. C., & Pringle, J. E. 1987, *ApJ*, 320, L87
 MacArthur, L. A., Courteau, S., Bell, E., & Holtzman, J. A. 2004, *ApJS*, 152, 175
 Macciò, A. V., Kang, X., & Moore, B. 2009, *ApJ*, 692, L109
 Macciò, A. V., Dutton, A. A., & van den Bosch, F. C. 2008, *MNRAS*, 391, 1940
 Madau, P., et al. 2008, *ApJ*, 689, L41
 Mo, H. J., Mao, S., & White, S. D. M. 1998, *MNRAS*, 295, 319
 Mo, H. J., Mao, S., & White, S. D. M. 1999, *MNRAS*, 304, 175
 Moore, B., Governato, F., Quinn, T., Stadel, J., & Lake, G. 1998, *ApJ*, 499, L5
 Moore, B., Ghigna, S., Governato, F., Lake, G., Quinn, T., Stadel, J., & Tozzi, P. 1999, *ApJ*, 524, L19
 Navarro, J. F., Frenk, C. S., & White, S. D. M. 1995, *MNRAS*, 275, 56
 Navarro, J. F., Frenk, C. S., & White, S. D. M. 1997, *ApJ*, 490, 493 (NFW)
 Purcell, C. W., Kazantzidis, S., & Bullock, J. S. 2009, *ApJ*, 694, L98
 Shen, S., et al. 2003, *MNRAS*, 343, 978
 Somerville, R. S., & Kolatt, T. S. 1999, *MNRAS*, 305, 1 (SK99)
 Stewart, K. R., Bullock, J. S., Wechsler, R. H., Maller, A. H., & Zentner, A. R. 2008, *ApJ*, 683, 597
 Taylor, J. E., & Babul, A. 2001, *ApJ*, 559, 716
 Taylor, J. E., & Babul, A. 2004, *MNRAS*, 348, 811
 Tegmark, M., et al. 2004, *ApJ*, 606, 702

- Thomas, D., Maraston, R. B., & de Oliveira, C. M. 2005, *ApJ*, 621, 673
- Tollerud, E. J., Bullock, J. S., Strigari, L. E., & Willman, B. 2008, *ApJ*, 688, 277
- Tóth, G., & Ostriker, J. P. 1992, *ApJ*, 389, 5
- Trujillo, I., et al. 2004, *ApJ*, 604, 521
- Trujillo, I., et al. 2006, *ApJ*, 650, 18
- Villalobos, A., & Helmi, A. 2008, *MNRAS*, 391, 1806
- Yoshii, Y., & Sommer-Larsen, J. 1989, *MNRAS*, 236, 779
- Zentner, A. R., & Bullock, J. S. 2003, *ApJ*, 598, 49 (ZB03)
- Zentner, A. R., Bullock, J. S., Kravtsov, A. V., & Wechsler, R. H. 2005, *ApJ*, 624, 505
- Zhang, J., Fakhouri, O., Ma, C.-P. 2008, *MNRAS*, 389, 1521